Studies on the wideband design of acousto-optic deflector using lithium niobate crystal

Jing Yang (杨 婧), Yanlei Gao (高艳磊), Jie Li (李 洁), Zhenjun Yang (杨振军), and Zhaoguang Pang (庞兆广)*

College of Physics Science and Information Engineering, Hebei Normal University, Shijiazhuang 050024, China

**Corresponding author: pangzhaoguang@163.com*

Received March 17, 2014; accepted May 3, 2014; posted online October 5, 2014

We present theoretical studies on the wideband design of bulk lithium niobate (LN) acousto-optic deflector (AOD) through the walk-off design of the ultrasonic vector, which satisfies the momentum match condition. The ultrasonic properties of LN crystal are studied by solving the Christopher equation and the reciprocal velocity curves in the operating planes *XOZ* and *YOZ* are systematically obtained. The calculation results show that the bandwidth of the AOD is highly dependent on the incident angle of light beam and the velocity of the ultrasonic waves, which show strict linear properties in the operating bandwidth. Furthermore, the dependence of the central frequency of the AOD on the angle of incident light and the ultrasonic velocity are also analyzed.

OCIS codes: 160.1050, 170.1065, 160.1190.
doi: 10.3788/COL201412.S21601.

Acousto-optic (AO) effect was first proposed by Brillouin in 1922[1] and experimentally demonstrated by Lucas *et al.*[2] in France, and Debye and Sears[3] in the United States. The basic principle of the AO deflector (AOD) is that the light beam is diffracted by the periodic distribution of the refractive index of the AO crystal, which is caused by the propagation of the ultrasonic waves in the crystal. The AOD devices can be used for the laser beam steering[4], imaging spectrometer[5], laser beam shaping[6], fringe projectors[7], multichannel communications[8], optical tweezers[9], and image scanners[10–13], The bandwidth of AO diffraction is one of the most important parameters of the AOD and the optimizing design of wideband operating mode is highly required for most applications.

We systematically studied the wideband design of the AOD through the walk-off design of the off-axis angle of the ultrasonic wave, where the bandwidth of the AOD can be determined by solving the Dixon equation of the anisotropic AO interaction, which indicates the geometrical relationships of the vectors of the diffractive optical wave, the ultrasonic wave, and the incident optical wave under the momentum match condition in the operating plane. The bandwidth features of the AOD in the operating planes of *XOZ* and *YOZ* are systematically calculated and the optimizing design of the wideband AOD is determined. Furthermore, the central frequency features of the AOD are also calculated and analyzed.

Anisotropic AO interaction can be described by the momentum match condition

$$\vec{k}_d = \vec{k}_i \pm \vec{K}, \tag{1}$$

where $\vec{k}_d$, $\vec{k}_i$ and $\vec{K}$ are the wave vectors of the diffraction light, the incident light, and the acoustic wave, the expressions of $\vec{k}_d$, $\vec{k}_i$ and $\vec{K}$ can be written as

$$k_i = \frac{2\pi n_i}{\lambda_0}, k_d = \frac{2\pi n_d}{\lambda_0}, K = \frac{2\pi}{\Lambda} = \frac{2\pi f}{V}, \tag{2}$$

where n_d is the refractive index of the diffractive light, n_i is the refractive index of the incident light, V is the velocity of the ultrasonic wave, f is the frequency of the ultrasonic wave, and λ_0 is the wavelength of the light wave.

The schematic diagram of the momentum match of lithium niobate (LN) anisotropic AO interaction in *XOZ* and *YOZ* planes is shown in Fig. 1

It is noted that θ_α is the angle between the vector of the ultrasonic wave and the *X*-axis and θ_d is the angle between the vector of diffractive light and the *Z*-axis. It can be observed from Fig. 1 that the refractive indexes of the incident and diffractive lights are different due to the change in polarization associated with the interaction. In our study the incident light is polarized perpendicularly to the *XOZ* (*YOZ*) plane in order to realize the wideband operating mode both for the +1 order diffraction and the −1 order diffraction. Thus the vector of the incident light is connected to the circular index curve (ordinary light) and the vector of the diffractive light is connected to the ellipse index curve (extraordinary light). At the same time, the acoustic wave vector connects the index curves of the incident and diffracted waves, as illustrated in Figs. 1(a) and (b).

From geometrical relationships of Figs. 1(a) and (b), the Dixon equation of LN anisotropic AO interaction can be derived as

$$\sin[\pm(\theta_a - \theta_i) = \frac{\lambda}{2n_o v}\left[f - \frac{v^2 n_o^2}{f\lambda^2}\left(\frac{n_e^2 - n_o^2}{n_e^2}\sin^2\theta_d\right)\right], \tag{3}$$

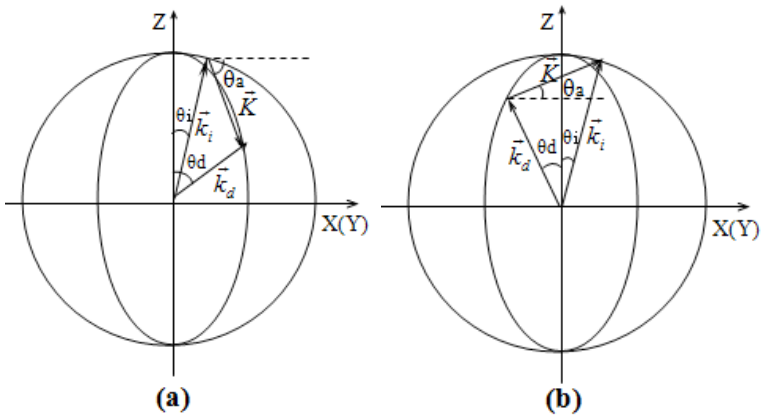

Fig. 1. Schematic diagram of the anisotropic AO interaction: (a) +1 order diffraction and (b) −1 order diffraction.

$$\sin[\pm(\theta_d - \theta_a)] = \frac{\lambda}{2n_o v}\left[f + \frac{n_o^2 v^2}{f\lambda^2}\left(\frac{n_e^2 - n_o^2}{n_e^2}\sin^2\theta_d\right)\right], \quad (4)$$

where the "±" means the +1 order diffraction and −1 order diffraction, respectively.

The acoustic property of LN crystal is determined by the Christoffel equation:

$$\left(\Gamma_{ij} - \rho v^2 \delta_{ij}\right)\cdot u_j = 0, \quad (5)$$

where $\Gamma_{ij} = L_{iJ}\, c_{iJ}\, L_{Ij}$, ρ is the density of the crystal and v is the velocity of the ultrasonic.

$$\delta_{ij} = \begin{cases} 0 & i = j \\ 1 & i \neq j \end{cases}, \quad (6)$$

$$L_{iJ} = \begin{pmatrix} l_x & 0 & 0 & 0 & l_z & l_y \\ 0 & l_y & 0 & l_z & 0 & l_x \\ 0 & 0 & l_z & l_y & l_x & 0 \end{pmatrix}, \quad (7)$$

where l_x, l_y, and l_i are the direction cosines of the vector of ultrasonic wave.

The velocity of ultrasonic wave in *XOZ* and *YOZ* planes can be obtained by extracting the eigenvector from the Christoffel equation, the reciprocal curves of the LN crystal is shown in Fig. 2.

It can be found that there are three reciprocal velocity curves in each operating plane. The curve mentioned with (1) is called the longitudinal wave, which leads to the isotropic AO interaction. The curves mentioned with (2) and (3) are named as sheared ultrasonic wave that can lead to the anisotropic AO effect. The values of the sheared ultrasonic waves along the *X*- and *Y*-axes are figured out as $v_{x1} = 3468$ m/s, $v_{x2} = 4020$ m/s, $v_{y1} = 3579$ m/s, and $v_{y2} = 4131$ m/s.

In order to realize the wideband design of LN anisotropic AOD by the walk-off design of the ultrasonic vector, the non-monotonicity condition of the $\theta_\alpha(f) \sim f$ curves in the operating bandwidth should be satisfied. Based on the calculation with Eqs. (3) and (4) it can be found that this non-monotonicity condition can be satisfied when $\theta_i \neq 0$. The $\theta_\alpha(f) \sim f$ curves under different incident angles θ_i are given in Figs. 3 (a) and (d).

In the actual design the off-axis angle of θ_α is set as $\theta_\alpha = \theta_{am} \pm \delta\theta_\alpha$ to realize the walk-off of the ultrasonic vector, where the θ_{am} is named the extremum angle and

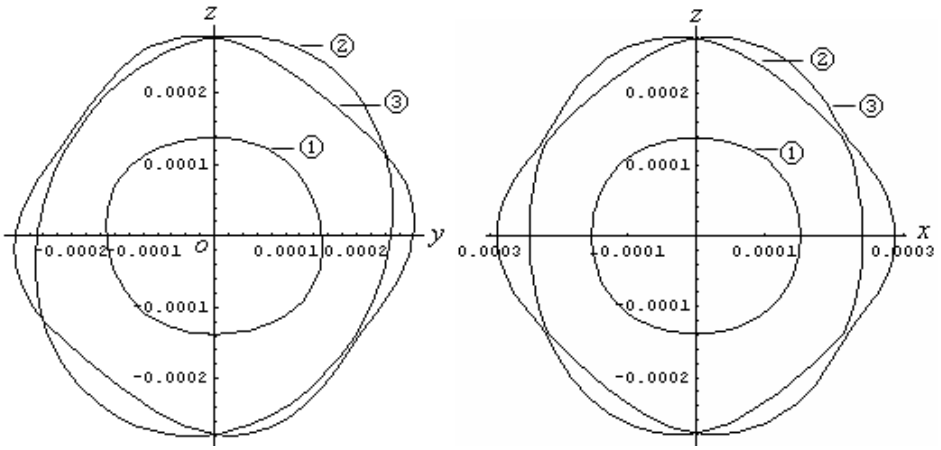

Fig. 2. The reciprocal velocity curves of LN crystal in (a) *XOZ* and (b) *YOZ* planes:

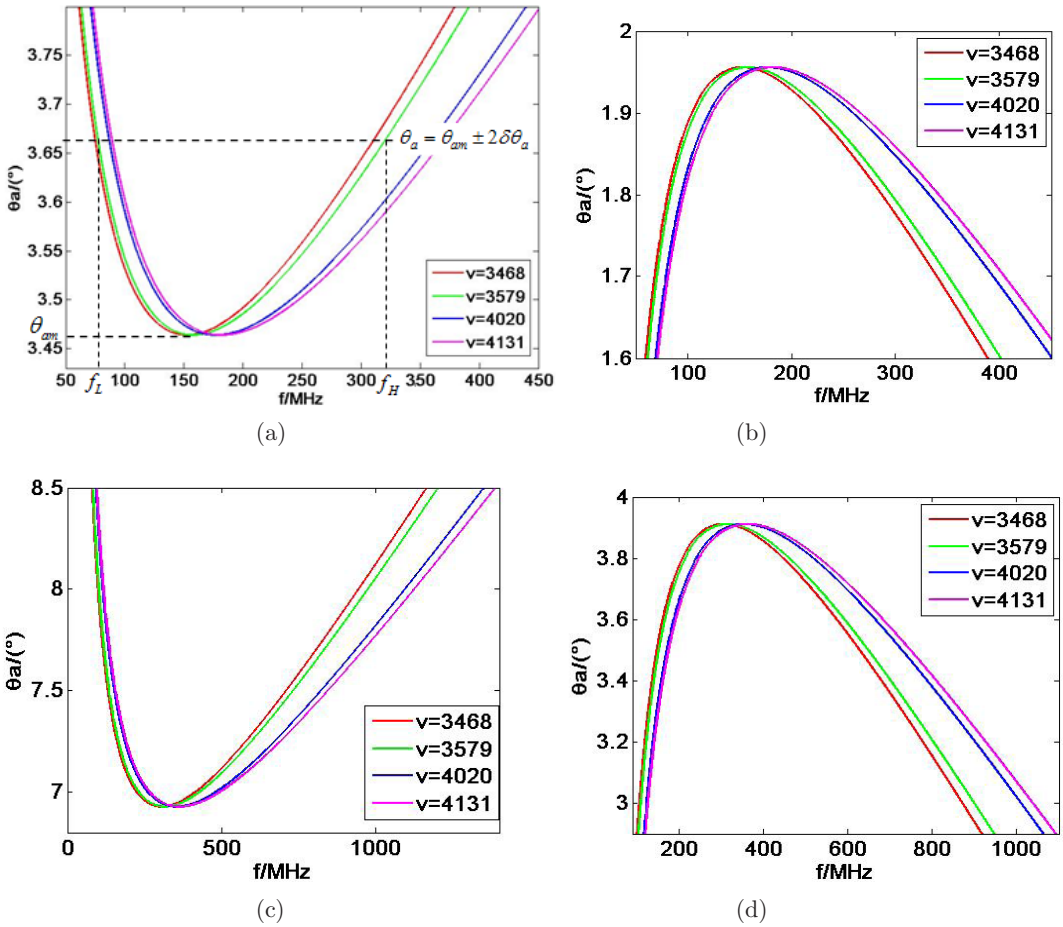

Fig. 3. $\theta_\alpha(f) \sim f$ curves under different incident angles and operating modes: (a) $\theta_i = 2.5°$, +1 order diffraction, (b) $\theta_i = 2.5°$, −1 order diffraction, (c) $\theta_i = 5°$, +1 order diffraction, and (d) $\theta_i = 5°$, −1 order diffraction.

can be determined by the theoretical calculation with the $\theta_\alpha(f) \sim f$ curve, the bandwidth of the AOD is calculated by the equation $\Delta f = f_H - f_L$, where f_H and f_L are the two frequencies that meet the $\theta_\alpha(f) \sim f$ curve for $\theta_\alpha = \theta_{am} \pm 2\delta\theta_\alpha$, as illustrated in Fig. 3(a). Herein, the dq_a is named the walk-off angle and usually set as 0.1, the "±" in the equation means the +1 order diffraction and −1 order diffraction, respectively. The central frequency is calculated by the equation of $f_c = f_H + f_L/2$.

From Figs. 3(a) and (d), the broadening of the AOD bandwidth with the increasing ultrasonic velocity and the incident angle can be observed qualitatively. Figure 4(a) shows the calculation results of the bandwidth at certain ultrasonic velocities under the incident angles of 2.5° and 5°, and Fig. 4(b) shows the results at certain incident angles at the ultrasonic velocities of 3467 and 4131 m/s.

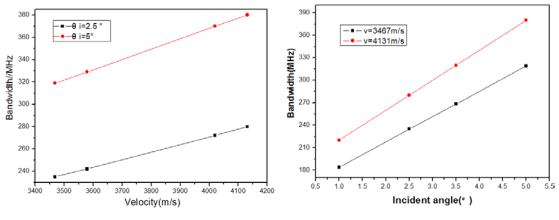

Fig. 4. The linearity relationships between: (a) the bandwidth and (b) the incident angle.

From Figs. 4(a) and (b) it can be clearly found that the AOD bandwidth is broadened linearly with the increase in the velocity and the incident angle θ_i. Furthermore, the gradient of the simulated lines also increase with the increase in the incident angle and the ultrasonic waves. Thus, we can conclude that under the same incident angle of θ_i, the optimum wideband design is to select the operating modes with the most fast ultrasonic wave to obtain the broad bandwidth.

The effects of the incident angle on the central frequency of the AOD are also studied under different sheared ultrasonic waves, and the calculation results for different velocities are shown in Figs. 5(a)–(d).

It can be observed from Figs. 5(a)–(d) that the simulated lines show strict linear relationship between the central frequency and the incident angle. Furthermore, it can also be found that the gradients of the linear relationship increases due to the increasing ultrasonic

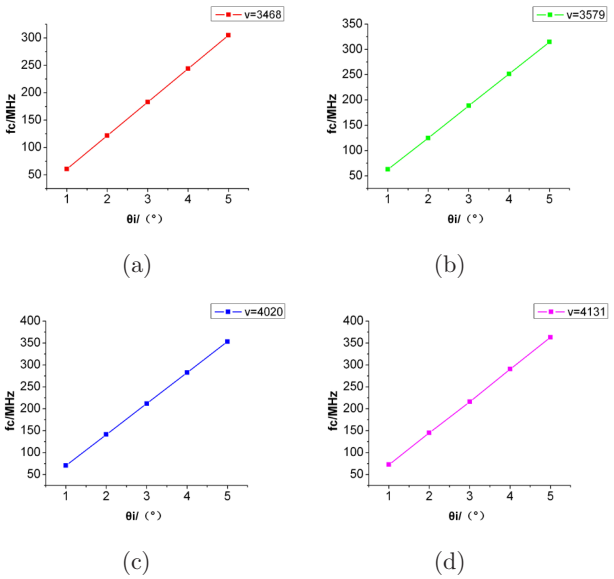

Fig. 5. The linearity relationships between the central frequency and the incident angle at different ultrasonic velocities: (a) $v = 3468$ m/s, (b) $v = 3579$ m/s, (c) $v = 4020$ m/s, and (d) $v = 4131$ m/s.

velocity, which shows similar properties as the feature the bandwidth analyzed in Fig. 4.

In conclusion, studies on the wideband design of LN AO are systematically carried out and the wideband design of the AOD is realized by the walk-off set of the ultrasonic vector, the bandwidths of the LN AOD are found to show strict linearity properties with the incident angle and with the ultrasonic velocities. Furthermore, the linearity properties of the central frequency with the incident angle and the ultrasonic velocity are also observed. Here we not only propose a new method for the wideband design of anisotropic AOD but also provide meaningful references for the design of novel devices based on the anisotropic AO diffraction.

This work was supported by the National Natural Science Foundation of China (Nos. 11374089 and 61308016), the Nature Science Foundation of Hebei Province (Nos. A2012205085, F2012205076, and A2012205023), and the Key Project of Hebei Education Department (No. ZD20131014).

References

1. L. Brillouin, Ann. Phys. (Paris) **17,** 88 (1922).
2. R. Lucas and P. Biquard, J. Phys. Rad. **3,** 464 (1932).
3. P. Debye and F. W. Sears, Proc. Natl Acad. Sci. (US) **18,** 409 (1932).
4. J. Mur, B. Kavcic, and I. Poberaj, App. Opt. **52,** 6506 (2013).
5. H. J. Zhao, P. W. Zhou, Y. Zhang, Z. Y. Wang, and S. G. Shi, Opt. Lett. **38,** 4120 (2013).
6. D. Trypogeorgos, T. Harte, A. Bonnin, and C. Foot, Opt. Express **21,** 24837 (2013).
7. S. Dupont, J. C. Kastelik, and M. Pommeray, IEEE/AMSE Trans. Mechatron. **15,** 557 (2010).
8. L. Zhao, Q. Zhao, J. Zhou, S. Tian, and H. Zhang, Ultrasonics **50,** 512 (2010).
9. K. C. Vermeulen, J. van Mameren, G. J. M. Stienen, E. J. G. Peterman, G. J. L. Wuite, and C. F. Schmidt, Rev. Sci. Instrum. **77,** 013704 (2006).
10. Y. Kremer, J. F. Léger, R. Lapole, N. Honnorat, Y. Candela, S. Dieudonné, and L. Bourdieu, Opt. Exp. **16,** 10066 (2008).
11. S. Yonghong, Q. Wan, and L. Honghai, Opt. Lett. **37,** 2532 (2012).
12. J. Runhua, Z. Zhenqiao, and L. Xiaohua, Rev. Sci. Instrum. **83,** 043709 (2012).
13. J. Qi, Y. H. Shao, and L. X. Liu, Opt. Lett. **38,** 1697 (2013).